



ChemSusChem

Chemistry–Sustainability–Energy–Materials

 **Chemistry
Europe**

European Chemical
Societies Publishing

Accepted Article

Title: Crystal-to-Crystal synthesis of photocatalytic MOFs for visible-light reductive coupling and mechanistic investigations

Authors: Julio Lloret-Fillol, Luis Gutiérrez, Suwendu Sekhar Mondal, Alberto Bucci, Noufal Kandoth, Eduardo C. Escudero-Adán, and Alexandr Shafir

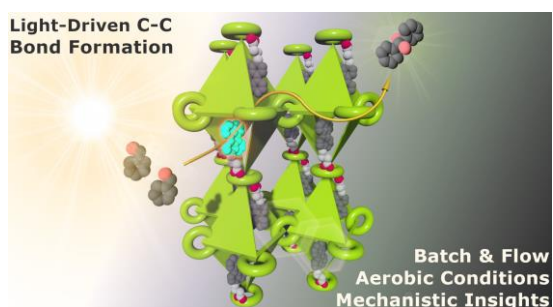
This manuscript has been accepted after peer review and appears as an Accepted Article online prior to editing, proofing, and formal publication of the final Version of Record (VoR). This work is currently citable by using the Digital Object Identifier (DOI) given below. The VoR will be published online in Early View as soon as possible and may be different to this Accepted Article as a result of editing. Readers should obtain the VoR from the journal website shown below when it is published to ensure accuracy of information. The authors are responsible for the content of this Accepted Article.

To be cited as: *ChemSusChem* 10.1002/cssc.202000465

Link to VoR: <https://doi.org/10.1002/cssc.202000465>

WILEY-VCH

Graphical abstract:



Dyes into crystals do not go with the flow:

Crystal-to-crystal post-functionalization of MOF-520 with perylene yield a photocatalytic active material. The functionalised MOF promoted by light, the reductive coupling of aromatic aldehydes, ketones and imines; even under aerobic conditions under batch and flow. The dyes into the highly regular X-ray-diffractive MOF behave like the homogeneous

systems in solution, which help to clarify the reaction mechanism.

KEYWORDS: MOF, Photoredox Catalysis, Crystal-to-Crystal, Pinacol Coupling, Flow.

Crystal-to-Crystal synthesis of photocatalytic MOFs for visible-light reductive coupling and mechanistic investigations

Luis Gutiérrez,^{a,✉} Suwendu Sekhar Mondal,^{a,✉} Alberto Bucci,^a Noufal Kandoth,^a Eduardo C. Escudero-Adán,^a Alexandr Shafir,^b and Julio Lloret-Fillol^{a,c,*}

^a Institute of Chemical Research of Catalonia (ICIQ), The Barcelona Institute of Science and Technology, Avinguda Païos Catalans 16, 43007 Tarragona, Spain

^b Institute of Advanced Chemistry of Catalonia (IQAC-CSIC), c/Jordi Girona 18-26, 08034, Spain.

^c Catalan Institution for Research and Advanced Studies (ICREA), Passeig Lluís Companys, 23, 08010, Barcelona, Spain

Email: jlloret@iciq.es

ABSTRACT:

Post-modification of reticular materials with well-defined catalysts is an appealing approach to produce new catalytic functional materials with improved stability and recyclability, but also to study the catalysis phenomena in confined spaces. A promising strategy to this end is the post-functionalization of crystalline and robust metal-organic frameworks (MOFs) exploiting the potential of crystal-to-crystal transformations for further the characterisation of catalysts. In this regard, two new photocatalytic materials, MOF-520-PC1 and MOF-520-PC2, are straightforwardly obtained by the post-functionalization of MOF-520 with perylene-3-carboxylic acid (PC1) and perylene-3-butyric acid (PC2). The single crystal-to-crystal transformation yielded the X-ray diffraction structure of catalytic MOF-520-PC1. The well-defined disposition of the perylenes inside the MOF served as suitable model systems to get insights into the photophysical properties and mechanism by combining steady-state, time-resolved and transient absorption spectroscopy. The resulting materials are active photoredox catalysts in the reductive dimerisation of aromatic aldehydes, benzophenones, and imines, under mild reaction conditions. Moreover, MOF-520-PC2 can be applied for synthesising gram-scale quantities of products in continuous-flow conditions under steady-state light irradiation. This work provides an alternative approach for the construction of well-defined metal-free MOF based catalysts.

INTRODUCTION.

Photoredox catalysis has emerged as a powerful synthetic alternative as compared to classical thermal organic transformations.^[1] An important family of photoredox catalysts (PCs) are based on Ir, Ru and Cu transition metals due to their robustness and long-lived MLCT excited states.^[1e,2] As a cost-effective alternative, organic dyes PCs such as benzophenones, cyanoarenes, quinolinium, pyrilium salts have emerged as promising photoredox catalysts based on earth-abundant elements.^[3] Additionally, simple perylene can also efficiently promote redox transformations under light irradiation.^[4]

A promising approach to further develop catalysts is to combine outstanding intrinsic activities of homogeneous systems with the chemical stability of heterogeneous ones by immobilisation of catalytic sites. In some cases, catalyst immobilisation leads to a reduction of performance due to the inaccessibility of active sites and mass transport issues. On the other hand, the recyclability and stability of heterogenised catalysts generally increase. Successful examples include the coordination of PCs on porous zeolites,^[5] polymers,^[6] and metal-organic frameworks (MOFs).^{[7],[8]} Among them, MOFs are versatile materials since they are built from organic bridging ligands and inorganic connecting points (referred as secondary building units or SBUs).¹⁰ Not only the large number of accessible SBUs,^[9] metalloligands,^[10] and organic linkers,^{[11],[12]} but also the post-modification by encapsulation of guest molecules offer a further possibility of functionalisation, such as the incorporation of photoactive molecules.^[13] As a result, the properties of the final material can be modulated to broaden the range of possible applications, from gas adsorption,^[14] sensing,^[15] light-emitting devices,^[16] biochemical systems^[17] to heterogeneous catalysis.^[18] Therefore, MOFs are unique to design earth-abundant metal-based single-site solid catalyst.^[18i] Still, only a limited number of MOFs have been reported to catalyse light-driven organic transformation,^[19] despite the wide variety of homogeneous photoredox catalyst counterparts.^[19] Those examples rely on demanding synthetic procedures, such as the synthesis of Ru(II) and Ir(III)-polypyridyl complex into UiO-type frameworks or metalloporphyrins MOFs,^[10] or the use of photoredox organocatalyst for direct synthesis of polymers^[11-12]

A pioneering work by Yaghi and co. demonstrated that the coordinative alignment (CAL) of a guest molecule to the MOF-520's SBU is an excellent methodology allowing the post-synthetic modification and determination of a single-crystal X-ray structure and absolute configuration of bound molecules.^[20] This crystal-to-crystal modification involves the replacement of the bridging formate ligands at the SBUs with guest molecules possessing either a carboxylate, phenol, diol, azolate, sulfur-containing oxoacid, and a phosphorus-containing oxoacid.^[20]

Inspired by these studies, we hypothesised the advantage of including functional guest molecules into MOF-520, such as photoredox catalysts. The coordination of the guest molecule into the SBU places the photoredox catalyst in a confined environment, which may allow for the crystallographic characterisation and therefore aiding into the mechanistic understanding. Another interesting aspect of the coordination of guest molecules into MOF-520 is that can be considered as isolated units and therefore acting as single-site catalysts in a heterogeneous material. In general, mechanistic studies of heterogeneous phases are more challenging than homogeneous ones. However, heterogeneous reticular materials, with well-defined single catalytic sites, may serve to clarify mechanistic aspect that otherwise is tough to address in a homogeneous phase. For instance, it could be useful to elucidate the active catalytic species in photoredox catalysts based on π -conjugated molecules. The tendency to form π -stacking aggregates in solution introduces an uncertainty like catalytic species since the dynamics of the excited states are very complex.^[21] In those systems, the catalytic activity can take place from the monomer, the dimer, larger aggregates, or from a combination of them.

As proof of concept, we have anchored two different photoredox catalysts (PCs) in MOF-520. Perylene-3-carboxylic acid (PC1) and perylene-3-butyric acid (PC2) reacted with MOF-520 and incorporated in the structure in a crystal-to-crystal transformation. The resulting MOFs (MOF-520-PC1 and MOF-520-PC2) showed photoredox catalytic activity for the C–C bond reductive dimerisation of aromatic aldehydes, ketones and imines, under mild reaction conditions. Diols and diamines obtained are structural motifs in natural products,^[22] pharmacologically active compounds, and auxiliaries in asymmetric syntheses.^[23] The reaction was also performed under continuous flow irradiation and aerobic conditions to generate bulk amount of desired products. Furthermore, the obtained MOF-520 based photocatalysts are suitable model systems to perform photophysical studies. The perylenes within the MOFs behave as single units, in contrast to the expected behaviour in the homogeneous phase. We also present the insights on the photocatalytic cycle obtained with the help of steady-state, time-resolved spectroscopic studies and transient absorption spectroscopic studies.

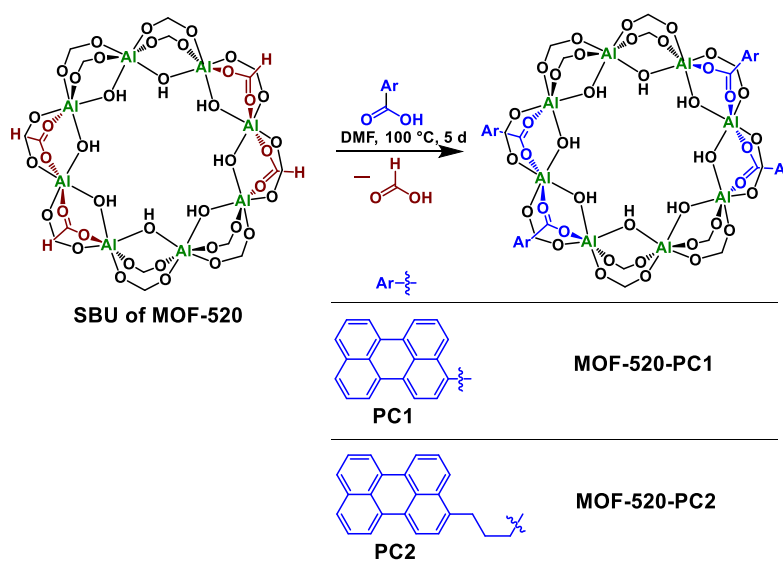
RESULTS AND DISCUSSION

Synthesis and structure determination:

Single crystals of MOF-520 were obtained in good yield following the procedure previously reported.^[20a] As previously reported, the X-ray analysis showed the SBUs ($[\text{Al}_8(\mu\text{-OH})_8(\text{HCOO})_4(\text{BTB})_4]$) constituted by a ring of eight aluminium octahedra shared corners through eight $\mu\text{-OH}$ s, twelve BTB (4,4',4''-benzene-1,3,5-triyl-tris(benzoate)) and four formate ligands, with wide window openings (13.7 Å) and cavities. Each BTB is connected to three SBUs

to form a three dimensional (3D) porous framework. The formates are exchangeable and offer anchoring points for molecules derivate with carboxylate acids.

The SBU was straightforwardly modified by incubating the crystalline white MOF-520 in DMF at 100 °C for five days in the presence of an excess amount of perylene-3-carboxylic acid (**PC1**) or perylene-3-butyrac acid (**PC2**) (Scheme 1 and see the Supporting Information (SI) for details). At the end of the reaction, dark-reddish crystals were severely washed with DMF and acetone and collected by filtration (Figure S1).



Scheme 1. Presentation of the crystal-to-crystal reaction by ligand exchange. Formate ligands are replaced by carboxylate derivate perylenes (**PC1** and **PC2**) into the SBU of MOF-520. Incoming perylene and outgoing formic acid are highlighted with red and blue colours, respectively.

The powder X-Ray diffraction (PXRD) pattern of the coloured MOF-520-PC1 and MOF-520-PC2 exhibited sharp diffraction peaks identical to the ones of the as-synthesized sample, indicating that the porous framework maintained the crystalline integrity (Figure 1a). Dinitrogen (N_2) adsorption/ desorption isotherms (77 K) of MOF-520, MOF-520-PC1, and MOF-520-PC2, indicate a decrease in porosity (Figure 1b), with Brunauer–Emmett–Teller (BET) surface areas determined to be 2438, 1448, and 1081 m^2/g , respectively. The loss of BET surface area is consistent with the steric bulk of guest perylene ligands residing in the pores of the MOF-520. These MOFs exhibited reversible type I sorption curves, which are characteristic of microporous materials.

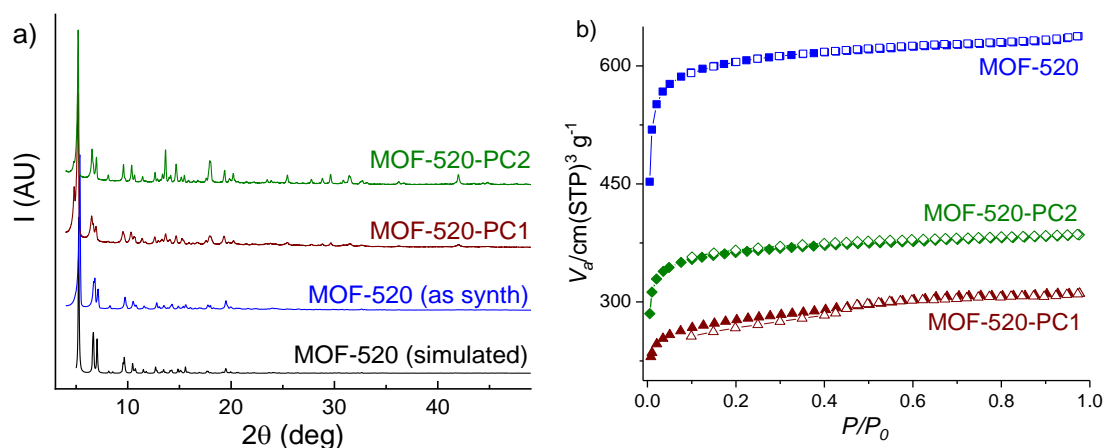


Figure 1. a) PXRD patterns and b) N₂ sorption isotherms at 77 K of MOF-520 (blue), MOF-520-PC1 (red), and MOF-520-PC2 (green). Adsorption and desorption branches are indicated in closed and open symbols, respectively.

Liquid-phase ¹H NMR spectroscopy of digested MOF-520-PC1 and MOF-520-PC2 samples was performed in order to quantify the amount of guest catalyst binding in the bulk samples. The samples (1 mg) were transferred to a GC vial. Deuterated dimethyl sulfoxide (d₆-DMSO) (0.4 mL) was added to the vial followed by the addition of 0.1 mL of NaOH (1 M in D₂O). The solution was sonicated for 5 min to digest the crystals. The vial was capped and placed in a preheated 120 °C oven for approved h to dissolve the crystals completely. The final clear solution was used for recording ¹H-NMR spectrum. The perylene incorporation was determined by the ratio between the perylene and BTB linker measured in the digestion mixture (Figure S2-S4). Based on above results, we observed the 44% and 71% of incorporation of PC1 and PC2, respectively, postulating the formulas [Al₈(μ-OH)₈(HCOO)₂(PC1)₂(BTB)₄] and [Al₈(μ-OH)₈(HCOO)(PC2)₃(BTB)₄], respectively.

Single crystal diffraction of MOF-520-PC1 (Figure 2) confirms the presence of PC1 ligand coordinated through the carboxylate bridging to two aluminium atoms (Figure S5a). The X-ray occupancy factor of PC1 ligand was 40%, in agreement with nearly 50% of formate replaced determined ¹H NMR. We speculate that the full replacement of formates by PC1 is not possible due to the rigidity and steric hindrance of PC1 as judged by the potential collision between PC1 neighbouring positions within the same SBU (Figure S5b). MOF-520-PC1 exhibits two types of ellipsoidal pores, formed from elongated arrangements of SBUs (Figure S5a). The first type is an octahedral pore of 10.01 Å × 10.01 Å × 23.23 Å, while the second type can accommodate an elongated tetrahedral of 5.89 Å × 5.89 Å × 6.21 Å (given the van der Waals radii of the nearest atoms).^[20a] A PLATON calculation indicates that the solvent-accessible void space of MOF-520-PC1 is approx. 6000 Å³, that accounts for ca. 50 % of the crystal volume (See SI animation

highlighting the MOF cavity, windows and PC1 included). In the case of the MOF-520-PC2, although the single crystal data collection was successful the detection of PC2, it was not possible the resolution of the structure, most probably be due to the high degree of freedom of the flexible $-(\text{CH}_2)_3$ -unit.

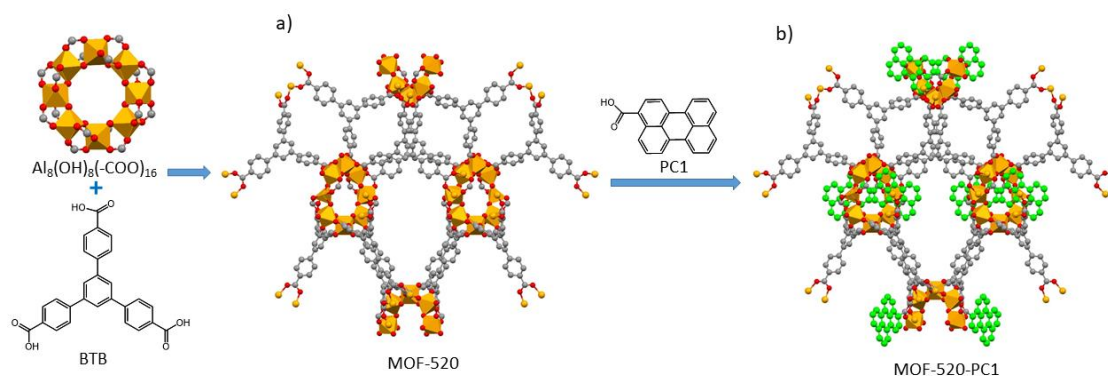


Figure 2. a) Synthesis of MOF-520 from Al-based SBUs and organic BTB linkers, Al-based SBU is orange polyhedral. b) The reaction of PC1 with MOF-520 leads to MOF-520-PC1. Atom colour scheme: C: grey; O: red; Al: orange; perylene: green; and H atoms are omitted for clarity.

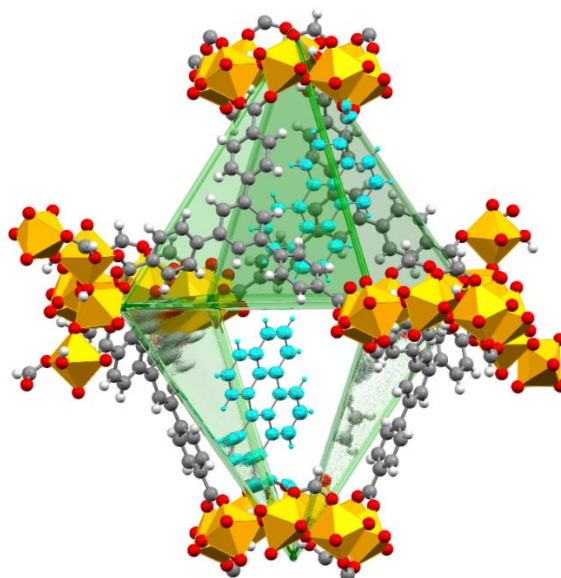


Figure 3. Representation of the X-ray single-crystal diffraction structure of MOF-520-PC1. The MOF cavity and framework ligands are emphasized with the green translucent plains. PC1 moieties are represented in blue ORTEP and Al-based SBUs in orange polyhedral.

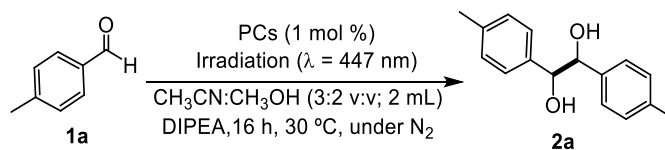
The strong coordination bond between Al^{3+} and the carboxylate groups, along with the high connectivity between the $[\text{Al}_8]$ clusters infers an expected of MOF-520-PC1 and MOF-520-PC2 stability under different conditions. In this regard, we tested the stability of dispersed MOF samples in acetone, tetrahydrofuran, methanol, acetonitrile, dichloromethane, and DMF for three

days at room temperature. After such a treatment, the material maintained the fully crystalline integrity as confirmed by PXRD (Figure S6 and S7).

Catalysis.

To proof the photocatalytic ability of the encapsulated PC inside the MOFs, we selected the light-driven pinacol coupling of a model substrate 4-methylbenzaldehyde (**1a**). We find that both suspension of MOF-520-PC1 or MOF-520-PC2 (0.5 mol %) in CH₃CN and after irradiation with visible light (447±20 nm) for 16 h in the presence of DIPEA under N₂ atmosphere, yielded the corresponding pinacol (**2b**) in low yields (9 % and 32 %, respectively). These results encourage us to optimise the conditions of the reaction (Table S2-S4).^[3a] After the optimising the solvent mixture (MeOH:CH₃CN, 3:2 v:v), the yield increase up to 74 and 82 % for MOF-520-PC1 and MOF-520-PC2, respectively, when using 1 mol % of MOF-520-PC. Loadings of 1 mol % of MOF-520-PC is substantially lower than previously used for homogeneous perylene organocatalysis (ca. 8-10%).^[3a] Blank experiments under dark, without DIPEA, or without PC (MOF-520-PC2) did not produce **2b** (Table S3), and MOF-520 (without PC) was inactive. Interestingly, the catalytic reaction mediated by MOF-520-PC2 was also effective under aerobic environment, giving a similar catalytic performance as under anaerobic conditions (Table S3). Reductive transformations under aerobic conditions are uncommon,^[24] and usually need to elaborate sophisticated strategies to avoid the reactivity of the O₂ with the reduced catalyst.^[25]

Following, we directly compared the MOF-520-PCs with the corresponding homogeneous PCs under the best reaction conditions (Table 1). Interestingly, the heterogeneous materials exhibit similar activity than homogeneous counterparts. These results suggested that most of the catalytic centres within the MOF-520-PCs are accessible and active or that the incorporation enhances the activity of the perylenes in the MOF structure. Besides, leaching experiments suggested that MOFs are robust and the primary source of the catalytic activity. The amount of PC1 and PC2 leach measured by UV-Vis absorption at the end of the catalytic run was only about 2.3 % and 1.4 % of PC1 and PC2 (Figure S9 and S10).

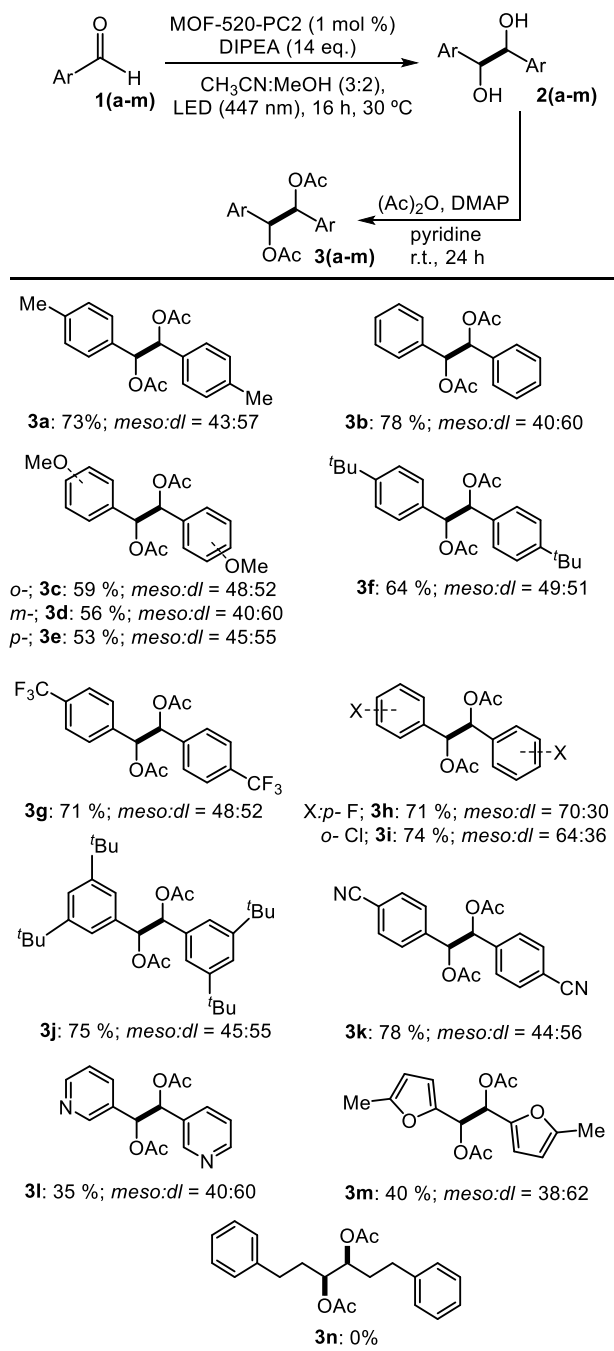
Table 1. Summary of control experiments for the reductive coupling reactions.

Photocatalyst (PC)	PC (mol %)	yield (%) ^a
PC1	0.5	68
PC2	0.5	63
PC1	2	75
PC2	3	81
MOF-520-PC1	0.9 (1.6) ^b	74
MOF-520-PC2	0.9 (2.8) ^b	82

Conditions: 4-methylbenzaldehyde (**1a**, 0.1 mmol), DIPEA (1.4 mmol) and different photocatalysts in $\text{CH}_3\text{CN}/\text{CH}_3\text{OH}$ (v:v = 3:2, 2 mL) at 30°C, under N_2 were irradiated for 16 h (LED 447 nm). ^a Yield is calculated by ¹H-NMR using 1,3,5-trimethoxybenzene, as an internal standard (I.S.). ^b The PC incorporation within the structure is 44% and 77% for PC1 and PC2, respectively. Therefore, it should be considered that the PC concentration is estimated to be about 1.6 mol % and 2.8 mol % for PC1 and PC2, respectively.

Following, we extended the scope to a broad range of aromatic aldehydes with electron-donating, electron-withdrawing and bulky substituents. MOF-520-PC2 was the chosen catalyst for the isolation of products because of the better yield. In order to facilitate the isolation of the products, the formed diols **2(a-m)** were converted into the corresponding diacetate **3(a-m)** using standard conditions (see SI). The formation of products was obtained from moderate to excellent yields (around 70%) under the optimised conditions (Table 2). Interestingly, heteroaromatic aldehydes **1l** and **1m** were found to be compatible with the reaction conditions, although it gave only from moderate to low yield. The developed methodology was not compatible with aliphatic aldehyde **1n**. Having outlined the scope for aldehydes, we next applied MOF-520-PC2 catalyst to benzophenones and imines without further optimisation (Table 3). In the case of imine reduction, up to 79% of yield was found. The limit of the catalytic system starts to appear in the coupling of more bulky substrates and the more challenging to reduce substrates, such as ketones and aliphatic aldehydes.^[26]

Table 2. Summary of the results obtained for the reductive coupling reactions of aromatic aldehydes, catalysed by MOF-520-PC2.

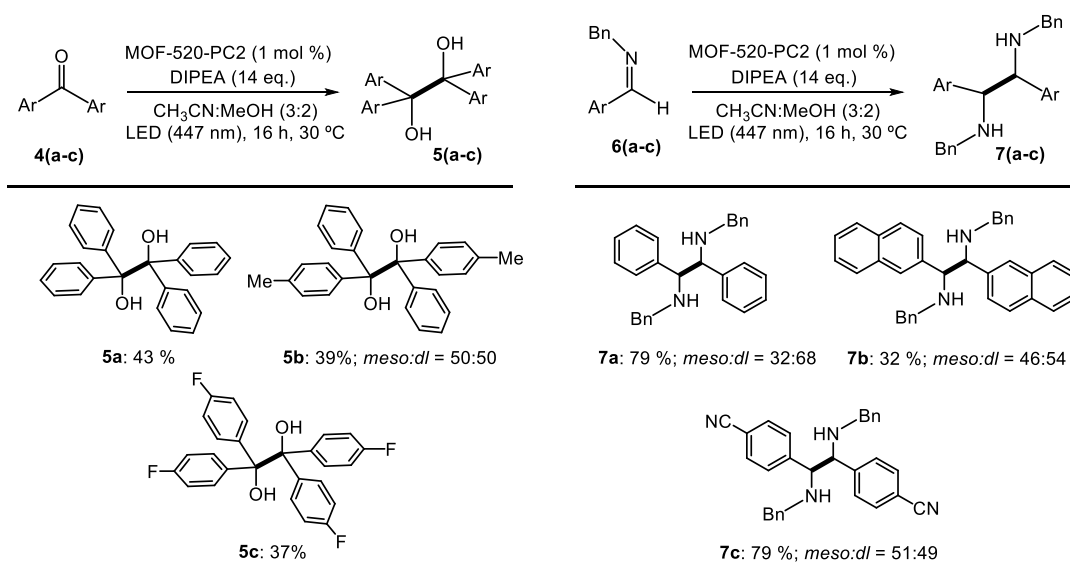


Reaction conditions: MOF-520-PC2 (1 mol%), aldehyde (0.1 mmol), DIPEA (1.4 mmol), in CH₃CN/CH₃OH (v:v = 3:2, 2 mL) at 30 °C, under N₂ during 16 h of irradiation (LED 447 nm). Yields are referred to isolated products; each substrate was run in three vials in parallel reactions that were combined after the end of the reaction for isolation.

On the other hand, although the significant advances produced in the pinacol coupling reaction,^[27] the intermolecular cross-pinacol coupling that produces a single cross-coupled 1,2-diol selectively still remains a challenge.^[28] Strategies to address the chemoselective control include pre-functionalization with stoichiometric quantities of metal salts, employing one coupling partner in large quantities, using highly functionalized carbonyl compounds,^[29] or exploiting differences in reactivity between coupling partners via an ionic mechanism.^[30] In this regard, to proof the effect of the photocatalysts encapsulation into the **MOF-520-PC2** into selectivity, we preformed the hetero-coupling of two different aldehydes, **1b** and **1j**, with marked differences in steric effects and compared with the homogeneous **PC2**.

The reactions were carried out using an equimolar mixture of the two aldehydes. Moreover, irradiated for 8 h to better appreciate the differences in reactivity. The crude of the reaction, without further manipulation, was analyzed by ¹H-NMR using an internal standard for quantification. In this way, the selectivity is not altered during the isolation procedure (**Table S7**). Although in both cases a mixture of homo-coupling (**2j**, **2b**) and hetero-coupling (**2o**) products were obtained there is a remarkable difference in the selectivity for the bulkier substrate **2j**. A homolytic product selectivity **2b/2j** value of 4.6 fold was obtained for **MOF-520-PC2**, while is 1.0 for **PC2**. This 4.6 fold increase for the **2b** formation versus **2j** suggests a size-exclusion effect of the cavities of **MOF-520-PC2**.

Table 3. Summary of the results obtained for the reductive coupling reactions of benzophenones and aromatic imines, catalysed by MOF-520-PC2.



Reaction conditions: MOF-520-PC2 (1 mol%), ketone or imine (0.1 mmol), DIPEA (1.4 mmol), CH₃CN/CH₃OH (v:v = 3:2, 2 mL) at 30 °C, under N₂ during 16 h of irradiation (LED 447 nm).

Yields referred to isolated products. Each substrate was run in two vials in parallel reactions that were combined after the end of the reaction for isolation.

Recycling in batch: MOF-520-PC2 can be easily separated and recovered from the reaction mixture through filtration. Therefore, we studied the potential recycling of the catalysts after catalysing the pinacol coupling of **1a**. After washing twice with methanol and acetone, the recycled MOF-520-PC2 was subjected to a following up catalytic run with the same substrate. The catalytic activity was maintained for the first two cycles (79 and 75 %) and dropped in the third one to 34 % of **2a** (Table S5). This reduction of the yield was accompanied by a significant reduction in the crystallinity of the catalyst, as confirmed by its PXRD patterns (Figure S11). We rationalise that the prolonged stirring used under the catalytic conditions may be the responsible for the structure degradation of MOF-520-PC2, which then diminish the catalytic activity since the catalytic sites are no longer reachable by the organic substrates.

Photocatalysis in flow: Taking advantage of the heterogeneous nature of MOF catalyst, we studied the potential use of MOF-520-PC2 as photocatalyst in flow.^{[31],[32]} Indeed, flow chemistry has many advantages, such as easy up-scaling and automatisation.^[33] However, the scarce light penetration is most probably the reason behind the few applications of photocatalytic transformation using heterogeneous materials under flow.

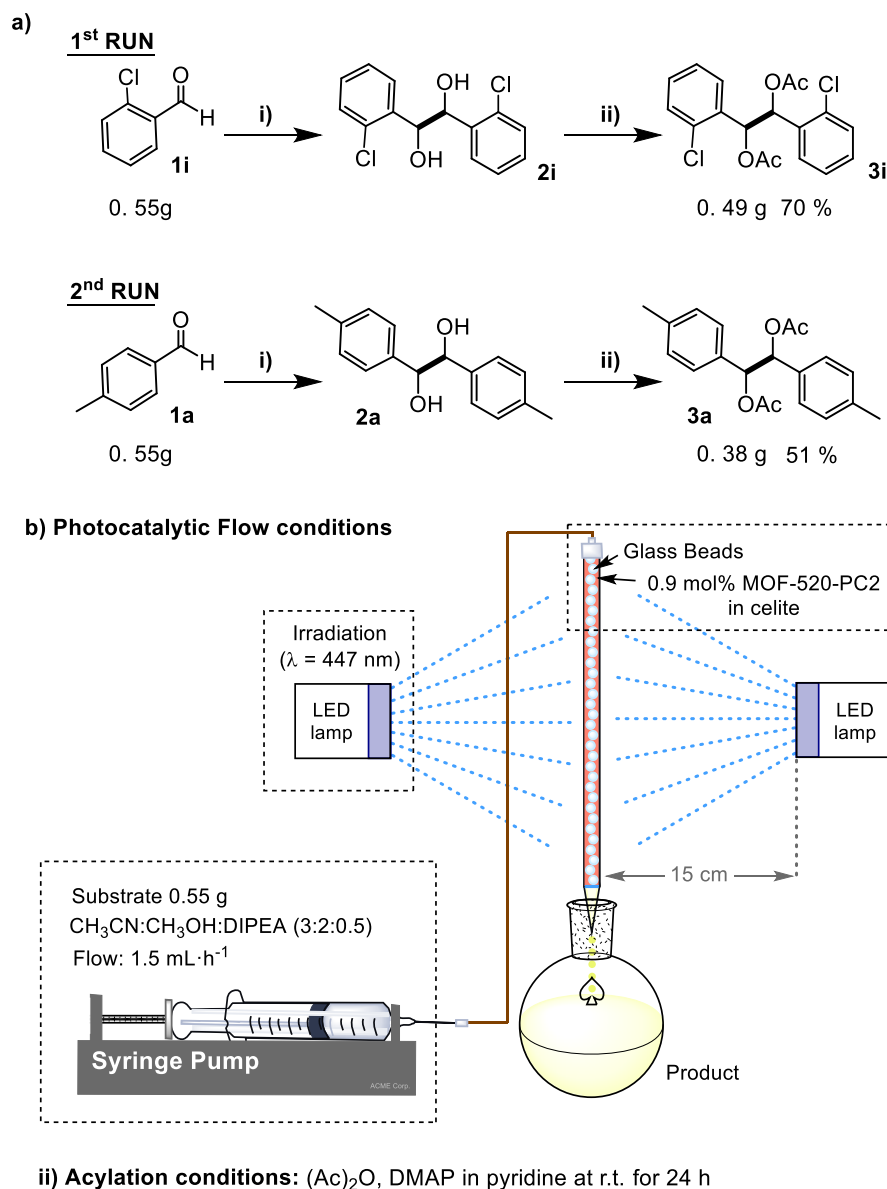


Figure 4. a) Consecutive photocatalytic reduction of aldehydes **1i** and **1a** to the corresponding pinacols in flow with the same MOF-520-PC2/celite® packed column. b) Schematics of the experimental setup.

The nature of the developed material (MOF-520-PC2) encouraged us to develop a heterogeneous photocatalytic system operative in flow. We selected prototype substrates with different electronic properties, **1i** and **1a**, for the testing. To set up the flow reactor, we prepared a 1 % dilution of the MOF-520-PC2 in celite® and directly packed into a column (20 x 0.6 cm) with glass beads to increase the light-harvesting of the photocatalyst (Figure 4, see SI for further details). The packing was carried out under aerobic conditions without any particular precaution. The reaction mixture contained the substrate and the electron donor under identical conditions to those already discussed optimised for batch reactions. The photoreactor was irradiated perpendicular to the

surface from two light sources (Kessil lamp 450 nm) at 180° one to each other. The first solution containing 0.55 g of **1i** was pumped through the photoreactor (flow rate of 1.5 mL·h⁻¹ Figure S12), followed by 0.55 g of **1a** after washing. Noteworthy, the sample preparation and the photoreactions were done under air atmosphere, further demonstrating the robustness of the catalytic system. As a result, the two consecutive 0.55 g scale reactions produced good overall isolated yields of products **3i** and **3a** (0.49 and 0.38 g corresponding to 70 and 51 % yield after two reactions, respectively, Figure 4), validating the effectiveness of the system.

Photophysical and electrochemical characterization.

To better understand the nature of the catalytic sites, we have investigated the photophysical and electrochemical properties of the as-synthesized MOFs and PCs.

First, optical spectroscopic studies to give insights into potential interactions between perylenes, or perylenes and the MOF matrix. Diffused reflectance spectra of solid PC1 and PC2 precursors (Figure S13a and S13b) showed a broad characteristic perylene monomer absorption band with a peak at about 430 nm.^[34] In both cases, encapsulation in the MOF-520 only induced minor changes in the absorbance, suggesting that the electronic structure of the PC are not essentially altered in the solid-state. Absorption and luminescence studies in solution or suspension in the case of MOFs were more informative regarding the potential aggregation processes (Figure 5 and S14). The UV-Vis absorption spectrum of PC1 and PC2 shows broad bands (360-470 nm). In the case of the PC1 the characteristic vibrational fine structure of the perylene is not resolved, even at concentrations as low as 1 μM, while in the case of PC2, the characteristic vibronic spectra of perylene monomers are present (1 – 25 μM). Presumably, the difference raised from the different capacity of PC1 and PC2 to form π -stacking structures, which is likely more favourable for PC1 since the formation of carboxylic acid homodimers duplicate the size of the π -conjugated structure (See Figure 5). This is in agreement with the fact that the presence of a base such as *N,N*-Diisopropylethylamine (DIPEA, 5 mM) resolves the characteristic vibronic spectra of perylene monomers for PC1, since it disrupts that formation of homodimers. The UV-Vis features of PC1 and PC2 are located in the visible region, without overlapping the MOF-520 absorption of the BTB linkers (276 nm), facilitating the analysis of the post-modified MOFs (Figure S14).

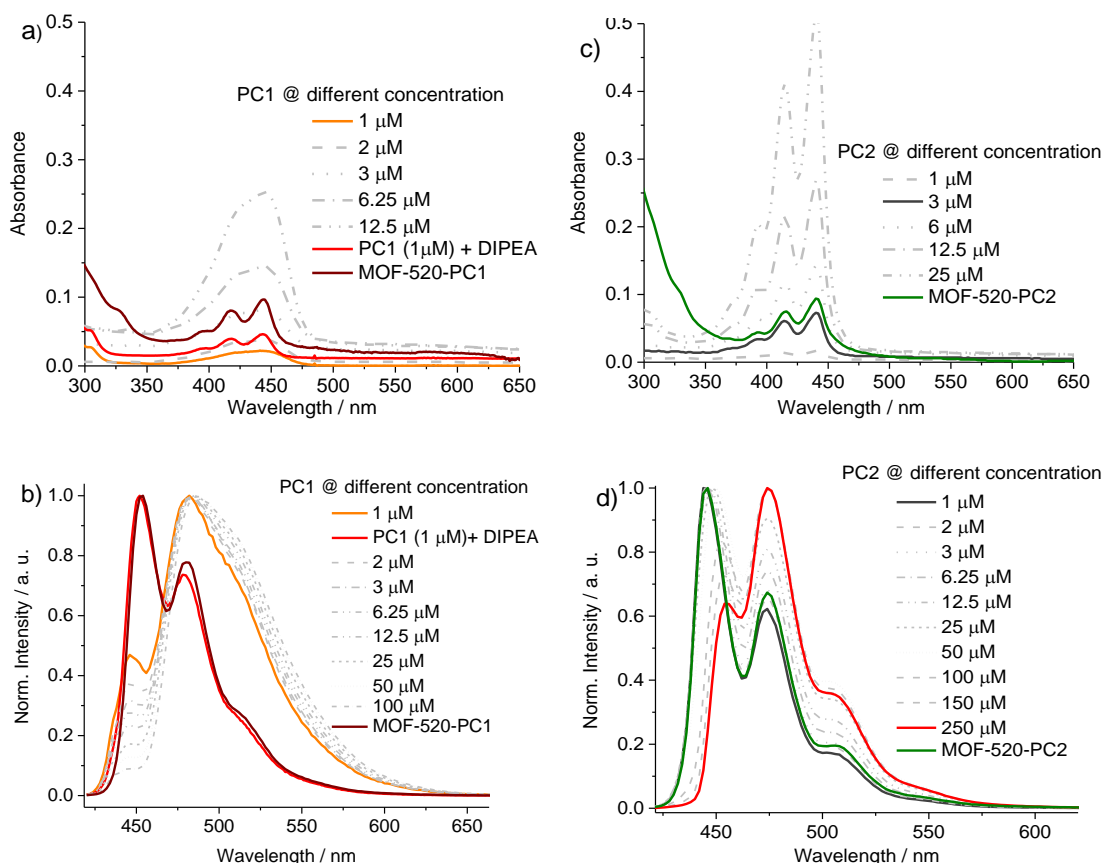


Figure 5. (a-b) Absorption and fluorescence spectra of PC1 measured upon increasing its concentration and further compared with a suspension of MOF-520-PC1 (1 mg/mL), (c-d) Absorption and fluorescence spectra of PC2 measured upon increasing its concentration and further compared with the same in the presence of DIPEA and MOF-520-PC2 (1 mg/mL) in suspension. Solvent CH_3CN , DIPEA (5 mM), $\lambda_{\text{exc}} = 410$ nm.

Interestingly, in the absorption spectra of the MOF-520-PCs, perylene vibronic features are present for both cases, suggesting negligible perylene – perylene interactions or MOF structure – perylene interactions. To further understand the aggregation behaviour of perylenes inside the MOF matrix, we also recorded fluorescence spectra of PCs in the concentration range from 1 to 100 μM , as well as MOF-520-PCs suspensions. Like in the UV-Vis absorption spectra, PC1 fluorescence spectra showed unresolved vibronic features, which appeared in the presence of DIPEA and perfectly matched to the spectrum of the suspended MOF-520-PC1. Also informative was the fluorescence spectra in the case of PC2 and MOF-520-PC2. While the concentration increases, the luminescence vibronic bands at 445 nm decrease and the feature at 475 nm rises, revealing an aggregation process between perylene units, which was not revealed in the studied UV-Vis spectra range. (Figure 5). Likewise in the UV-Vis, the fluorescence spectrum of MOF-520-PC2 matches with that of PC2 only at low concentration (1 μM of photocatalyst), indicating that PC2 behaves as a monomer inside of the MOF-520.^[35]

Cyclic voltammetry (CV) experiments showed apparent differences between perylene precursors. The first reduction wave of PC2 is shifted by 340 mV to more negative potentials concerning PC1 ($E_{\text{PC2}}^0 = -1.80$ V and $E_{\text{PC1}}^0 = -1.45$ V, respectively). All redox values are given vs SCE otherwise notified (Table 4, Figure S13c). Although the CVs of the MOFs follow a similar trend than the perylene precursors, the interpretation is not straightforward. The CV of the MOF-520 shows two reduction waves that shifted to positive and negative redox potentials in MOF-520-PC1 and MOF-520-PC2, respectively (Figure S13d). We noticed that the extension of the shifts depends on the perylene. The shift was more significant in the case of MOF-520-PC1, where the perylene is electronically connected to the carboxylate and then to the aluminium centres. Conversely, for MOF-520-PC2, the perylene – Al centres are electronically disconnected by an alkyl spacer, and barely affects the redox process of the MOF.^[34] Nevertheless, since the absorption spectra and fluorescence do not suffer essential changes, we estimate the redox potentials of PCs within the MOF would not significantly deviate respect to the free PCs. Therefore, we hypothesize that the redox difference between the two materials can be ascribed as the main factor of the differences in catalysis.

Finally, we characterised the excited states by time-correlated single-photon counting in solid-state (Figure 6, and Table S8). In both cases, the multiexponential lifetime decay of PCs is similar to the MOF-520-PCs (Table 4), being the slowest $\tau_{1/2}$ about 6 ns for PC1 and 8 ns for PC2.^{[36],[35a],[37]} This result together with the previous ones are in agreement with the fact that both PCs behave as isolated units inside the MOF-520.

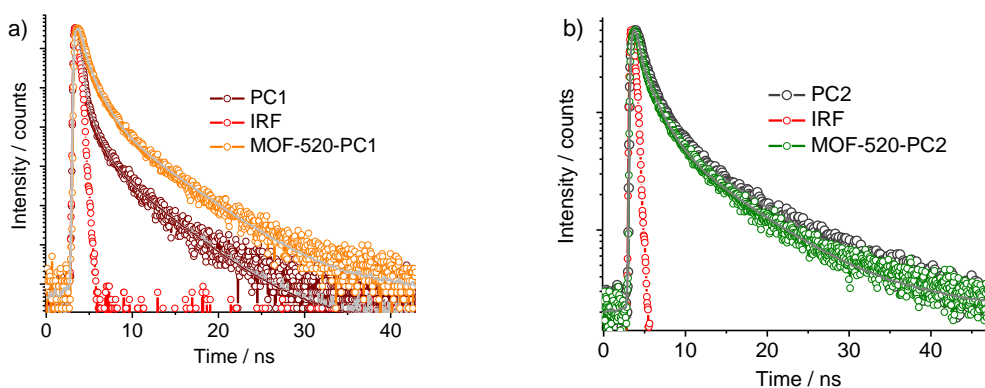


Figure 6. Normalised solid-state lifetime decay of a) PC1, MOF-520-PC1, and b) PC2, MOF-520-PC2 measured by time-correlated single-photon counting and its exponential fits. $\lambda_{\text{ex}} = 470$ nm laser, $\lambda_{\text{em}} = 560$ nm. (IRF = instrument response function from the laser source).

Mechanistic studies.

To get insights into the reductive coupling reaction of aldehydes, we examined key steps of the catalytic cycle with the help of steady-state, time-resolved fluorescence quenching studies and transient spectroscopy experiments. To this end, we have focused the efforts on the prototype reaction of **1a** with MOF-520-PC2 under suspension, in the absence and presence of DIPEA. As presented above, the perylene PC2 inside the MOF-520 behaves as a monomer as judged by the absorption and emission spectra (Figure S15, S17).

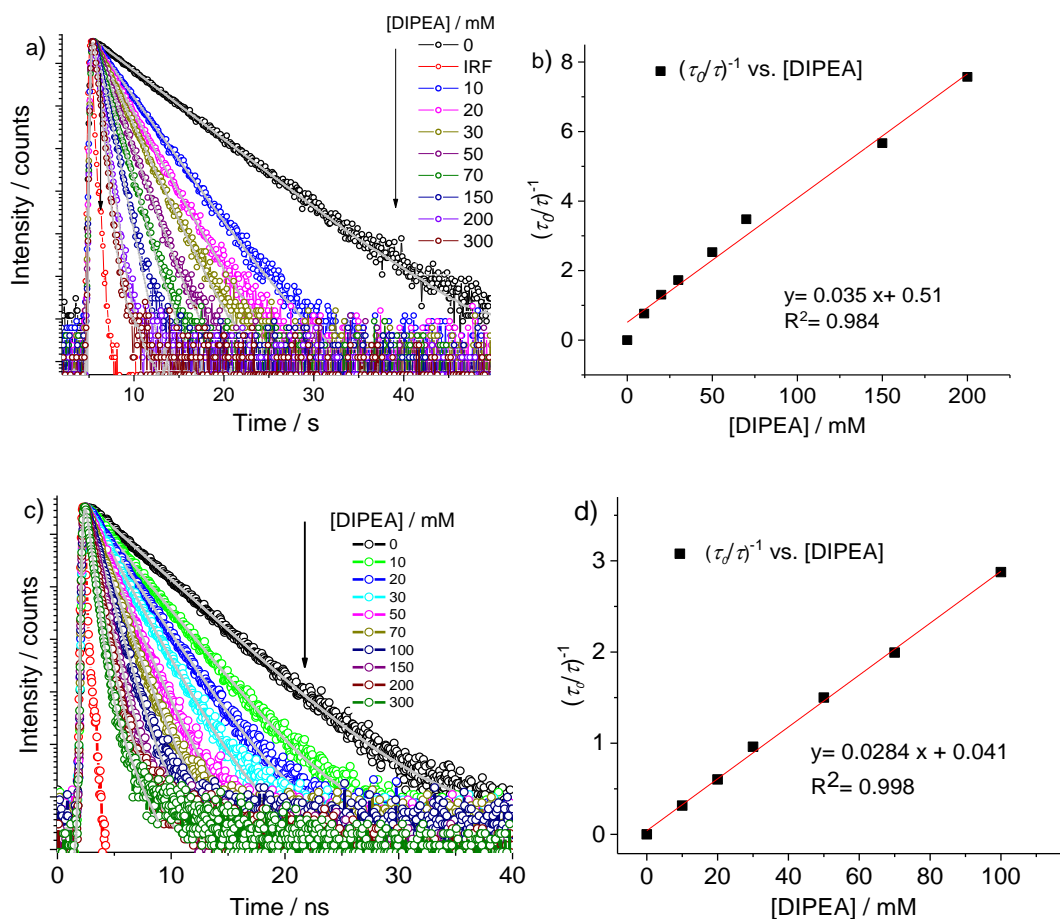


Figure 7. a) Titration lifetime decay of MOF-520-PC1 (a) and MOF-520-PC2 (c) with DIPEA in $\text{CH}_3\text{CN}/\text{CH}_3\text{OH}$ solvent mixture (v:v = 3:2, 2 mL). $\lambda_{\text{ex}} = 405$ nm laser, $\lambda_{\text{em}} = 460$ nm. Stern-Volmer quenching analysis of the lifetimes' changes as a function of [DIPEA] for MOF-520-PC1 (b) and MOF-520-PC2 (d). The sample prepared as fine suspension after ball milling, cell path length 1 cm, $T = 25$ °C.

Table 4. Summary of the redox processes and excited-state lifetimes in solution.

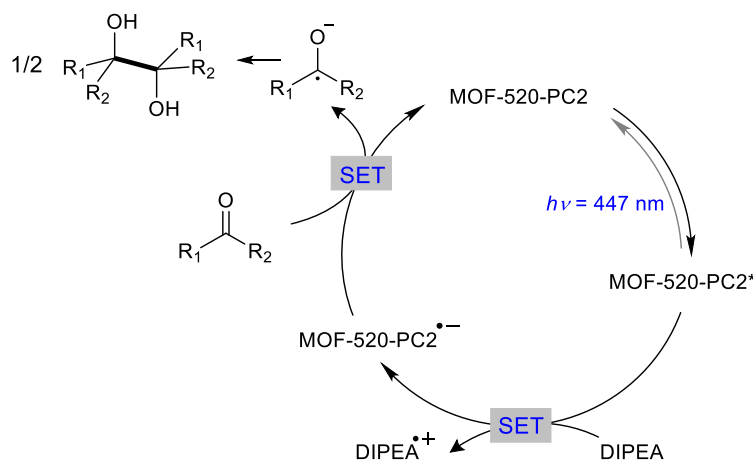
Sample	λ_{abs}^a	λ_{em}^b	τ_l^c	$E_{1/2}^{(0/-)}$	$E^{(*/-)}$
	[nm]	[nm]	[ns]	[SCE]	
PC1	442	452	4.5	-1.45	1.25
PC2	440	446	4.2	-1.80	1.0
MOF-520	275	390	3.5	-	-
MOF-520-PC1	445	454	6	-	-
MOF-520-PC2	440	448	5.2	-	-

^a Values obtained from the maximum absorption peak; ^b values obtained from the maximum fluorescence peak; ^c lifetime obtained from the single exponential function fit at the λ_{em} . Absorption and fluorescence spectra are collected CH₃CN/CH₃OH (v:v = 3:2).

The lifetime of the MOF-520-PC2* excited state was long enough to be quenched by the DIPEA as observed by the fluorescence (Figure S15c-d) and excited-state lifetime quenching studies (Figure 7c-d). Similar bimolecular quenching rate constants (k_q) were obtained by time-correlated single-photon counting for MOF-520-PC1 ($6.0 \pm 0.3 \cdot 10^9 \text{ M}^{-1}\text{s}^{-1}$, Table S9 and see SI for calculation details) and for MOF-520-PC2 ($5.9 \pm 0.3 \cdot 10^9 \text{ M}^{-1}\text{s}^{-1}$, Table S10). When studying **1a** as a quencher, we could not observe quenching at concentration relevant for catalysis (Figure S16). Redox values of DIPEA and PC2* suggests that a single electron transfer (SET) between them is thermodynamically feasible ($E_{(\text{DIPEA})}^0 = 0.72 \text{ V}^{[38]}$ and $E_{(\text{PC2/PC2}^*)} = 1.0 \text{ V vs SCE}$, Figure S17b,d). Likewise, a SET from DIPEA to MOF-520-PC2* should also be thermodynamically feasible.^[39] Nevertheless, the formation of the radical anion of the photosensitiser can be observed by millisecond transient absorption spectroscopy. Indeed, in the case of PC2, the PC2* excited state follows the formation of the radical anion PC2⁻ in the presence of DIPEA (Figure S18a) with a clear absorption peak at 570 nm. Monitoring the radical anion at 570 nm presented a biexponential decay time of *ca.* 0.75 and 3.6 ms (Table S11), which can be rationalized as recombination in ms-time scale. Under the same condition but in the presence of **1a** the decays are reduced to 0.44 and 3.0 ms (Table S11).

Likewise, in the case of MOF-520-PC2 the evolution of the radical anion can be followed at 570 nm in the presence of DIPEA, but with faster decay time than in the case of the PC2 in solution ($\langle \tau \rangle = 0.25 \text{ ms}$). By adding **1a** to the same cuvette, the intensity of the signal at 570 nm is reduced

to more than half, suggesting a SET between the radical anion by **1a**. (Figure S18d). Therefore, the proposed mechanism of the photocatalytic reductive coupling reaction starts with the excitation of the PC ($\lambda = 447$ nm), which undergoes reductive quenching with DIPEA to afford MOF-520-PC^{•-}. The successive SET to the substrate results in the reduction of the carbonyl group, followed by the C-C homocoupling reaction (Scheme 2).^[26]



Scheme 2. Proposed mechanism of visible-light-driven reductive coupling reaction of aromatic aldehydes, acetophenones, and imines using MOF-520-PC2 photoredox catalyst.

CONCLUSION

In the present work, we reported a straightforward post-synthetic transformation of MOF-520 with two different substituted perylene molecules introducing a photoredox functionality to the material. As judged by the redox potential, the differences in catalytic activity between the two materials can be ascribed to the redox potential differences between the PCs reduced state, being PC2 more reducing than PC1. The new heterogeneous organo-photocatalysts revealed efficient light-driven reductive coupling of aldehydes, ketones and imines, to give 1,2-diols and 1,2-diamines, with similar catalytic activity to the homogeneous counterpart, but with recyclable capacity. Moreover, continuous flow photocatalytic conditions highlight the potential by proving gram scale catalytic transformation and reusability. Combining steady-state and time-resolved spectroscopy revealed that immobilised perylenes at the MOF-520 act as an isolated unit, and therefore the catalytic activity could be exclusively ascribed to perylene monomer, whereas in homogeneous phase the potential aggregation of perylenes complicates the assignment of the real catalytic active species. We envision that this study will open new perspectives in the design of heterogeneous photoredox catalysts by further developments on photocatalytic active materials based on the straightforward crystal-to-crystal transformation of MOF-520 as well as potential derived light-driven organic transformations under flow.

ASSOCIATED CONTENT

Supporting Information.

Figures, tables, text, and CIF files giving crystal data, experimental details, and the catalysis results.

The crystal structure depositing number for MOF-520-PC1 is CCDC-1972303.

AUTHOR INFORMATION

Author Contributions

The manuscript was written through the contributions of all authors. / All authors have given approval to the final version of the manuscript. [‡] This authors contributed equally.

Notes

The authors declare no competing financial interest.

ACKNOWLEDGMENT

We thank the ICIQ Foundation, the European Research Foundation for project ERC-2014-CoG 648304 (J.L.-F.), MINECO (CTQ2016-80038-R; J.L.-F.) and AGAUR 2017-SGR-1647 (J.L.-F.). S.S.M. and N.K. thank Marie-Curie COFUND and JyC for postdoctoral scholarships, respectively.

REFERENCES

- [1] a) K. L. Skubi, T. R. Blum, T. P. Yoon, *Chem. Rev.* **2016**, *116*, 10035-10074; b) B. König, *Eur. J. Org. Chem.* **2017**, *2017*, 1979-1981; c) T. P. Yoon, M. A. Ischay, J. Du, *Nat. Chem.* **2010**, *2*, 527; d) L. Marzo, S. K. Pagire, O. Reiser, B. König, *Angew. Chem. Int. Ed.* **2018**, *57*, 10034-10072; e) C. R. Stephenson, T. P. Yoon, D. W. MacMillan, *Visible Light Photocatalysis in Organic Chemistry*, John Wiley & Sons, **2018**; f) L. Buzzetti, G. E. M. Crisenza, P. Melchiorre, *Angew. Chem. Int. Ed.* **2019**, *58*, 3730-3747.
- [2] a) C. K. Prier, D. A. Rankic, D. W. C. MacMillan, *Chem. Rev.* **2013**, *113*, 5322-5363; b) O. Reiser, G. Kachkovskiy, V. Kais, P. Kohls, S. Paria, M. Pirtsch, D. Rackl, H. Seo, **2013**; c) A. Hossain, A. Bhattacharyya, O. Reiser, *Science* **2019**, *364*, eaav9713; d) D. M. Arias-Rotondo, J. K. McCusker, *Chem. Soc. Rev.* **2016**, *45*, 5803-5820; e) T. Koike, M. Akita, *Inorg. Chem. Front.* **2014**, *1*, 562-576; f) O. S. Wenger, *Coord. Chem. Rev.* **2015**, *282-283*, 150-158; g) Q. M. Kainz, C. D. Matier, A. Bartoszewicz, S. L. Zultanski, J. C. Peters, G. C. Fu, *Science* **2016**, *351*, 681; h) A. Sagadevan, V. P. Charpe, A. Ragupathi, K. C. Hwang, *J. Am. Chem. Soc.* **2017**, *139*, 2896-2899; i) S. Paria, O. Reiser, *ChemCatChem* **2014**, *6*, 2477-2483; j) Y. Zhang, M. Schulz, M. Wächter, M. Karnahl, B. Dietzek, *Coord. Chem. Rev.* **2018**, *356*, 127-146.
- [3] a) N. A. Romero, D. A. Nicewicz, *Chem. Rev.* **2016**, *116*, 10075-10166; b) C. Stephenson, T. Yoon, *Acc. Chem. Res.* **2016**, *49*, 2059-2060; c) M. Silvi, E. Arceo, I. D. Jurberg, C. Cassani, P. Melchiorre, *J. Am. Chem. Soc.* **2015**, *137*, 6120-6123; d) B. Schweitzer-Chaput, M. A. Horwitz, E. de Pedro Beato, P. Melchiorre, *Nat. Chem.* **2019**, *11*, 129-135; e) J. C. Theriot, C. H. Lim, H. Yang, M. D. Ryan, C. B. Musgrave, G. M. Miyake, *Science* **2016**, *352*, 1082-1086; f) B. G. McCarthy, R. M. Pearson, C.-H. Lim, S. M. Sartor, N. H. Damrauer, G. M. Miyake, *J. Am. Chem. Soc.* **2018**, *140*, 5088-5101; g) T.-Y. Shang, L.-H. Lu, Z. Cao, Y. Liu, W.-M. He, B. Yu, *Chem. Commun.* **2019**, *55*, 5408-5419; h) O. S.

- Wenger, *J. Am. Chem. Soc.* **2018**, *140*, 13522-13533; i) C. B. Larsen, O. S. Wenger, *Chem. Eur. J.* **2018**, *24*, 2039-2058.
- [4] a) S. Okamoto, K. Kojiyama, H. Tsujioka, A. Sudo, *Chem. Commun.* **2016**, *52*, 11339-11342; b) S. Okamoto, R. Ariki, H. Tsujioka, A. Sudo, *The Journal of Organic Chemistry* **2017**, *82*, 9731-9736.
- [5] a) M. Silva, *J. Hazard. Mater.* **2012**, v. 233-234, pp. 79-88-2012 v.2233-2234; b) M. Silva, M. E. Azenha, M. M. Pereira, H. D. Burrows, M. Sarakha, C. Forano, M. F. Ribeiro, A. Fernandes, *Applied Catalysis B: Environmental* **2010**, *100*, 1-9.
- [6] a) A. Corma, H. Garcia, *Chem. Commun.* **2004**, 1443-1459; b) Z. J. Wang, S. Ghasimi, K. Landfester, K. A. I. Zhang, *Chem. Mater.* **2015**, *27*, 1921-1924; c) W.-J. Yoo, S. Kobayashi, *Green Chem.* **2014**, *16*, 2438-2442.
- [7] Y. Liu, G. Zhu, B. Ge, H. Zhou, A. Yuan, X. Shen, *CrystEngComm* **2012**, *14*, 6264-6270.
- [8] a) H.-C. J. Zhou, S. Kitagawa, *Chem. Soc. Rev.* **2014**, *43*, 5415-5418; b) J. Liu, L. Chen, H. Cui, J. Zhang, L. Zhang, C.-Y. Su, *Chem. Soc. Rev.* **2014**, *43*, 6011-6061; c) K. Sumida, D. L. Rogow, J. A. Mason, T. M. McDonald, E. D. Bloch, Z. R. Herm, T.-H. Bae, J. R. Long, *Chem. Rev.* **2012**, *112*, 724-781.
- [9] a) K. G. M. Laurier, F. Vermoortele, R. Ameloot, D. E. De Vos, J. Hofkens, M. B. J. Roeffaers, *J. Am. Chem. Soc.* **2013**, *135*, 14488-14491; b) D. Wang, R. Huang, W. Liu, D. Sun, Z. Li, *ACS Catal.* **2014**, *4*, 4254-4260; c) Y. Zhang, J. Guo, L. Shi, Y. Zhu, K. Hou, Y. Zheng, Z. Tang, *Sci. Adv.* **2017**, *3*, e1701162.
- [10] a) C. Wang, Z. Xie, K. E. deKrafft, W. Lin, *J. Am. Chem. Soc.* **2011**, *133*, 13445-13454; b) X. Yu, S. M. Cohen, *Chem. Commun.* **2015**, *51*, 9880-9883; c) Y. Fang, X. Li, F. Li, X. Lin, M. Tian, X. Long, X. An, Y. Fu, J. Jin, J. Ma, *J. Power Sources* **2016**, *326*, 50-59; d) J. A. Johnson, X. Zhang, T. C. Reeson, Y.-S. Chen, J. Zhang, *J. Am. Chem. Soc.* **2014**, *136*, 15881-15884.
- [11] P. Wu, C. He, J. Wang, X. Peng, X. Li, Y. An, C. Duan, *J. Am. Chem. Soc.* **2012**, *134*, 14991-14999.
- [12] L. Zeng, T. Liu, C. He, D. Shi, F. Zhang, C. Duan, *J. Am. Chem. Soc.* **2016**, *138*, 3958-3961.
- [13] a) D. Shi, C. He, B. Qi, C. Chen, J. Niu, C. Duan, *Chem. Sci.* **2015**, *6*, 1035-1042; b) X. Wang, W. Lu, Z.-Y. Gu, Z. Wei, H.-C. Zhou, *Chem. Commun.* **2016**, *52*, 1926-1929.
- [14] a) J.-R. Li, R. J. Kuppler, H.-C. Zhou, *Chem. Soc. Rev.* **2009**, *38*, 1477-1504; b) K. Tan, S. Zuluaga, E. Fuentes, E. C. Mattson, J.-F. Veyan, H. Wang, J. Li, T. Thonhauser, Y. J. Chabal, *Nat. Comm.* **2016**, *7*, 13871.
- [15] a) L. E. Kreno, K. Leong, O. K. Farha, M. Allendorf, R. P. Van Duyne, J. T. Hupp, *Chem. Rev.* **2012**, *112*, 1105-1125; b) J. J. Gassensmith, J. Y. Kim, J. M. Holcroft, O. K. Farha, J. F. Stoddart, J. T. Hupp, N. C. Jeong, *J. Am. Chem. Soc.* **2014**, *136*, 8277-8282; c) P. Wu, Y. Liu, Y. Liu, J. Wang, Y. Li, W. Liu, J. Wang, *Inorg. Chem.* **2015**, *54*, 11046-11048; d) F.-Y. Yi, D. Chen, M.-K. Wu, L. Han, H.-L. Jiang, *ChemPlusChem* **2016**, *81*, 675-690.
- [16] a) Y. Cui, Y. Yue, G. Qian, B. Chen, *Chem. Rev.* **2012**, *112*, 1126-1162; b) J. Yu, Y. Cui, C.-D. Wu, Y. Yang, B. Chen, G. Qian, *J. Am. Chem. Soc.* **2015**, *137*, 4026-4029; c) B. Chen, L. Wang, Y. Xiao, F. R. Fronczek, M. Xue, Y. Cui, G. Qian, *Angew. Chem. Int. Ed.* **2009**, *48*, 500-503.
- [17] a) H. Zheng, Y. Zhang, L. Liu, W. Wan, P. Guo, A. M. Nyström, X. Zou, *J. Am. Chem. Soc.* **2016**, *138*, 962-968; b) C. Doonan, R. Riccò, K. Liang, D. Bradshaw, P. Falcaro, *Acc. Chem. Res.* **2017**, *50*, 1423-1432.
- [18] a) Y.-B. Huang, J. Liang, X.-S. Wang, R. Cao, *Chem. Soc. Rev.* **2017**, *46*, 126-157; b) V. Pascanu, G. González Miera, A. K. Inge, B. Martín-Matute, *J. Am. Chem. Soc.* **2019**, *141*, 7223-7234; c) A. Dhakshinamoorthy, Z. Li, H. Garcia, *Chem. Soc. Rev.* **2018**, *47*, 8134-8172; d) N. Huang, K. Wang, H. Drake, P. Cai, J. Pang, J. Li, S. Che, L. Huang, Q. Wang, H.-C. Zhou, *J. Am. Chem. Soc.* **2018**, *140*, 6383-6390; e) N. Huang, S. Yuan, H. Drake, X. Yang, J. Pang, J. Qin, J. Li, Y. Zhang, Q. Wang, D. Jiang, H.-C. Zhou, *J. Am. Chem. Soc.* **2017**, *139*, 18590-18597; f) Z. Li, A. W. Peters, A. E. Platero-Prats, J. Liu, C.-W. Kung, H. Noh, M. R. DeStefano, N. M. Schweitzer, K. W. Chapman, J. T. Hupp, O. K.

- Farha, *J. Am. Chem. Soc.* **2017**, *139*, 15251-15258; g) J. Liu, J. Ye, Z. Li, K.-i. Otake, Y. Liao, A. W. Peters, H. Noh, D. G. Truhlar, L. Gagliardi, C. J. Cramer, O. K. Farha, J. T. Hupp, *J. Am. Chem. Soc.* **2018**, *140*, 11174-11178; h) T. Zhang, K. Manna, W. Lin, *J. Am. Chem. Soc.* **2016**, *138*, 3241-3249; i) T. Drake, P. Ji, W. Lin, *Acc. Chem. Res.* **2018**, *51*, 2129-2138.
- [19] a) X. Yu, L. Wang, S. M. Cohen, *CrystEngComm* **2017**, *19*, 4126-4136; b) L. Zeng, X. Guo, C. He, C. Duan, *ACS Catal.* **2016**, *6*, 7935-7947; c) W. Tu, Y. Xu, S. Yin, R. Xu, *Adv. Mater.* **2018**, *30*, 1707582; d) C. Xu, R. Fang, R. Luque, L. Chen, Y. Li, *Coord. Chem. Rev.* **2019**, *388*, 268-292; e) Y.-Y. Zhu, G. Lan, Y. Fan, S. S. Veroneau, Y. Song, D. Micheroni, W. Lin, *Angew. Chem. Int. Ed.* **2018**, *57*, 14090-14094; f) R. Xu, Z. Cai, G. Lan, W. Lin, *Inorg. Chem.* **2018**, *57*, 10489-10493; g) T. Zhang, W. Lin, *Chem. Soc. Rev.* **2014**, *43*, 5982-5993; h) J.-L. Wang, C. Wang, W. Lin, *ACS Catal.* **2012**, *2*, 2630-2640.
- [20] a) S. Lee, E. A. Kapustin, O. M. Yaghi, *Science* **2016**, *353*, 808-811; b) F. Gándara, H. Furukawa, S. Lee, O. M. Yaghi, *J. Am. Chem. Soc.* **2014**, *136*, 5271-5274; c) E. A. Kapustin, S. Lee, A. S. Alshammari, O. M. Yaghi, *ACS Cent. Sci.* **2017**, *3*, 662-667; d) X. Pei, H.-B. Bürgi, E. A. Kapustin, Y. Liu, O. M. Yaghi, *J. Am. Chem. Soc.* **2019**, *141*, 18862-18869.
- [21] a) R. E. Cook, B. T. Phelan, R. J. Kamire, M. B. Majewski, R. M. Young, M. R. Wasielewski, *J. Phys. Chem. A* **2017**, *121*, 1607-1615; b) F. M. Winnik, *Chem. Rev.* **1993**, *93*, 587-614; c) A. Aster, G. Licari, F. Zinna, E. Brun, T. Kumpulainen, E. Tajkhorshid, J. Lacour, E. Vauthey, *Chem. Sci.* **2019**, *10*, 10629-10639; d) J. R. Lakowicz, **2006**; e) Y. Huang, J. Xing, Q. Gong, L.-C. Chen, G. Liu, C. Yao, Z. Wang, H.-L. Zhang, Z. Chen, Q. Zhang, *Nat. Comm.* **2019**, *10*; f) F. Ito, Y. Kogasaka, K. Yamamoto, *J. Phys. Chem. B* **2013**, *117*, 3675-3681; g) A. Furube, M. Murai, Y. Tamaki, S. Watanabe, R. Katoh, *J. Phys. Chem. A* **2006**, *110*, 6465-6471; h) Y. Nakamura, T. Nakazato, T. Kamatsuka, H. Shinokubo, Y. Miyake, *Chemistry – A European Journal* **2019**, *25*, 10571-10574; i) M. Bonchio, Z. Syrgiannis, M. Burian, N. Marino, E. Pizzolato, K. Dirian, F. Rigodanza, G. A. Volpato, G. La Ganga, N. Demitri, S. Berardi, H. Amenitsch, D. M. Guldi, S. Caramori, C. A. Bignozzi, A. Sartorel, M. Prato, *Nat. Chem.* **2018**, *11*, 146-153; j) A. S. Weingarten, R. V. Kazantsev, L. C. Palmer, M. McClendon, A. R. Koltonow, A. P. S. Samuel, D. J. Kiebal, M. R. Wasielewski, S. I. Stupp, *Nat. Chem.* **2014**, *6*, 964-970; k) X. Feng, P. Liao, J. Jiang, J. Shi, Z. Ke, J. Zhang, *ChemPhotoChem* **2019**, *3*, 1014-1019; l) E. Peris, *Chem. Commun.* **2016**, *52*, 5777-5787; m) S. Ibáñez, M. Poyatos, E. Peris, *Angew. Chem. Int. Ed.* **2018**, *57*, 16816-16820; n) S. Ibáñez, M. Poyatos, E. Peris, *Organometallics* **2017**, *36*, 1447-1451; o) S. Ibáñez, E. Peris, *Chemistry – A European Journal* **2019**, *25*, 8254-8258.
- [22] a) K. C. Nicolaou, J. J. Liu, Z. Yang, H. Ueno, E. J. Sorensen, C. F. Claiborne, R. K. Guy, C. K. Hwang, M. Nakada, P. G. Nantermet, *J. Am. Chem. Soc.* **1995**, *117*, 634-644; b) M. Nazaré, H. Waldmann, *Angew. Chem. Int. Ed.* **2000**, *39*, 1125-1128.
- [23] a) R. M. Archer, M. Hutchby, C. L. Winn, J. S. Fossey, S. D. Bull, -- **2015**, *71*, 8838-8847; b) R. A. Kleinnijenhuis, B. J. J. Timmer, G. Lutteke, J. M. M. Smits, R. de Gelder, J. H. van Maarseveen, H. Hiemstra, *Chemistry – A European Journal* **2016**, *22*, 1266-1269; c) H. Huo, C. Fu, K. Harms, E. Meggers, *J. Am. Chem. Soc.* **2014**, *136*, 2990-2993.
- [24] a) A. Call, C. Casadevall, F. Acuña-Parés, A. Casitas, J. Lloret-Fillol, *Chem. Sci.* **2017**, *8*, 4739-4749; b) D. W. Wakerley, E. Reisner, *Energy Environ. Sci.* **2015**, *8*, 2283-2295.
- [25] N. Plumeré, O. Rüdiger, A. A. Oughli, R. Williams, J. Vivekananthan, S. Pöller, W. Schuhmann, W. Lubitz, *Nat. Chem.* **2014**, *6*, 822.
- [26] M. Nakajima, E. Fava, S. Loescher, Z. Jiang, M. Rueping, *Angew. Chem. Int. Ed.* **2015**, *54*, 8828-8832.
- [27] X.-F. Duan, J.-X. Feng, G.-F. Zi, Z.-B. Zhang, -- **2009**, *2009*, 277-282.
- [28] a) T. Hirao, in *Metal Catalyzed Reductive C–C Bond Formation: A Departure from Preformed Organometallic Reagents* (Ed.: M. J. Krische), Springer Berlin Heidelberg, Berlin, Heidelberg, **2007**, pp. 53-75; b) B. S. Terra, F. Macedo, Jr., *ChemInform* **2012**, *43*.

- [29] a) R. L. Danheiser, A. L. Helgason, *J. Am. Chem. Soc.* **1994**, *116*, 9471-9479; b) J. H. Freudenberger, A. W. Konradi, S. F. Pedersen, *J. Am. Chem. Soc.* **1989**, *111*, 8014-8016.
- [30] M. Takeda, A. Mitsui, K. Nagao, H. Ohmiya, *J. Am. Chem. Soc.* **2019**, *141*, 3664-3669.
- [31] a) A. Sachse, R. Ameloot, B. Coq, F. Fajula, B. Coasne, D. De Vos, A. Galarneau, *Chem. Commun.* **2012**, *48*, 4749-4751; b) V. Pascanu, P. R. Hansen, A. Bermejo Gómez, C. Ayats, A. E. Platero-Prats, M. J. Johansson, M. À. Pericàs, B. Martín-Matute, *ChemSusChem* **2015**, *8*, 123-130.
- [32] D. Cambié, C. Bottecchia, N. J. W. Straathof, V. Hessel, T. Noël, *Chem. Rev.* **2016**, *116*, 10276-10341.
- [33] C. Sambigiò, T. Noël, *Trends in Chemistry* **2019**.
- [34] J. Merz, A. Steffen, J. Nitsch, J. Fink, C. B. Schürger, A. Friedrich, I. Krummenacher, H. Braunschweig, M. Moos, D. Mims, C. Lambert, T. B. Marder, *Chem. Sci.* **2019**, *10*, 7516-7534.
- [35] a) A. K. Chaudhari, J.-C. Tan, *Nanoscale* **2018**, *10*, 3953-3960; b) M. D. Allendorf, C. A. Bauer, R. K. Bhakta, R. J. T. Houk, *Chem. Soc. Rev.* **2009**, *38*, 1330-1352; c) I. A. Fedorov, Y. N. Zhuravlev, V. P. Berveno, *The Journal of Chemical Physics* **2013**, *138*, 094509.
- [36] M. Müller, A. Devaux, C.-H. Yang, L. De Cola, R. A. Fischer, *Photochemical & Photobiological Sciences* **2010**, *9*, 846-853.
- [37] C. Dietl, H. Hintz, B. Rühle, J. Schmedt auf der Günne, H. Langhals, S. Wuttke, *Chemistry – A European Journal* **2015**, *21*, 10714-10720.
- [38] G. J. Barbante, N. Kebede, C. M. Hindson, E. H. Doeven, E. M. Zammit, G. R. Hanson, C. F. Hogan, P. S. Francis, *Chemistry – A European Journal* **2014**, *20*, 14026-14031.
- [39] a) A. K. Pal, C. Li, G. S. Hanan, E. Zysman-Colman, *Angew. Chem. Int. Ed.* **2018**, *57*, 8027-8031; b) J. S. Beckwith, B. Lang, J. Grilj, E. Vauthey, *The Journal of Physical Chemistry Letters* **2019**, *10*, 3688-3693.

TOC

